A multiscale approach to simulate vacuum drying of a packed bed of spray-frozen particles

COMSOL
CONFERENCE
2023 MUNICH

A multiscale approach to simulate vacuum drying of a packed bed of spray-frozen particles

L. Stratta, M. B. Adali, A. A. Barresi, G. Boccardo, A. Marcato, R. Tuccinardi, R. Pisano
Department of Applied Science and Technology, Politecnico di Torino, Torino, Italy.

Abstract

Preservation of biopharmaceuticals by spray freeze-drying is of great interest as it involves gentle drying and can be easily integrated with continuous manufacturing strategies. The drying of packed beds have been extensively studied experimentally, but a detailed mathematical model of such systems is still missing. The intrinsic multiscale nature of the phenomenon, i.e. drying of porous particles randomly stacked in porous beds, poses a number of challenges that previous studies failed to address. The objective of this work is to present the implementation on COMSOL Multiphysics of a new model, describing the drying of packed beds of frozen particles through the concept of a diffused interface. The simulations of a single particle at the micro-scale are used to inform the model of the packed bed at the macro-scale. The specific example of the drying of particles in a vial was used as a case study.

The macroscopic domain, composed of the glass vial and the packed bed, was constructed as a 2D axisymmetric geometry. The Heat transfer in porous media and Transport of diluted species in porous media modules were used to solve the heat and mass transport equations in the packed bed, while only the heat transfer was considered for the glass domain. In the packed bed, the Dusty-Gas Model (DGM) was implemented defining the diffusion and the convection terms in the pre-built transport equations. An additional Species source was added in the bed volume to account for the ice sublimation (or condensation) from the particles. This source term was determined based on the local fluid- and thermo-dynamics conditions and on the sublimation kinetic parameter, vs, which was determined from the simulations at the micro-scale. The sublimation thermal effect was accounted for adding a Heat source to the domain, calculated multiplying the aforementioned mass generation and the latent heat of sublimation. Finally, with the Domain ODEs and DAEs, the sublimation flux was integrated over time to obtain the sublimated ice and the local frozen fraction (S) of the bed. The diffused interface results from the distribution of the frozen fraction in the bed.

At the micro-scale, a single particle was simulated to obtain vs. The particle was divided in two domains, i.e. dried and frozen layer, and the interface motion was determined solving the Stephan problem in the Deformed geometry module. In the dried layer, the vapor mass transport was solved using the Darcy's law model. The kinetic parameter, vs, was determined integrating the sublimating mass flux over the interface surface and dividing the result by the driving force. Multiple simulations with different particle porosities were performed and the evolution of vs(S) was exported to the macroscopic simulation as interpolation functions.

The results show that this model predicts well the drying behavior of packed beds of frozen particles, distinguishing between scenarios in which either the bed or the particles porosity limits the mass transport, and predicting the development of multiple diffused sublimation fronts, as was theorized in the past.

Keywords: Spray freeze drying; diffused interface; multiscale; particles.

Introduction

Spray freeze-drying (SFD) is a pivotal downstream process widely employed in the pharmaceutical industry. It serves to preserve biopharmaceutical products with a limited shelf-life in liquid solutions and that lack the necessary temperature stability for conventional hot drying methods. In SFD, the targeted solution is atomized and rapidly frozen utilizing a cryogenic fluid, which can be in liquid or vapor form. Subsequently, the particles are collected, typically into vials or trays, and dried under vacuum conditions. The gentle drying conditions preserve the drug's activity, and the fine porous powder remains stable at ambient temperatures for extended periods. Despite extensive experimental investigation on the SFD process, a detailed model describing the drying behavior of the porous bed is still missing. The absence of such a precise mathematical model hampers the pharmaceutical industry's ability to optimize the process and choose the most suitable drying conditions. Although a few models have been proposed in the literature[1], [2], they all fall short in depicting the actual physical changes the system undergoes, consequently yielding only approximations.

To address this gap, our work[3] proposes a multiscale pseudo-homogeneous model, employing the concept of a diffused interface to simulate the drying behavior of packed beds composed of frozen particles. Ice sublimation occurs within the entire

system and the local water partial pressure dictates the sublimation rate. While a physical sublimation interface is present within individual particles, no distinct segregation is defined within the packed bed. However, the separation between frozen and dried regions at the macro-scale can be inferred through a more or less steep gradient in the intensive variable S, indicating the local frozen fraction. The model at the vial- and particle-scale was implemented using COMSOL Multiphysics, while the determination of the packed bed structure was achieved through combination of experimental evidence and computational models.

Description of the numerical model at the macroscopic scale

In this work, the model was applied to the specific case of vials, commonly used in the pharmaceutical industry, but the equations are generally valid and can be implemented on any kind of packed bed, with the necessary boundary conditions modifications.
Exploiting the axial symmetry of the vials, we simulated the system as a 2D-axisymmetric geometry, as illustrated in Figure 1.

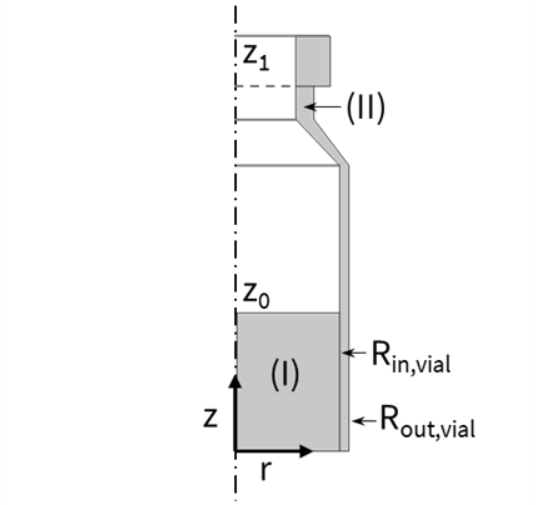

Figure 1. *Schematic of the packed bed of particles (I) contained within a vial (II). The axis of rotation is depicted as the dash-dot line.*

The *Heat transfer in porous media* and *Transport of diluted species in porous media* modules were used to solve the heat and mass transport equations in the system.

Heat transfer

In the glass domain (II), only the heat transfer equations were solved and the material properties were defined to simulate the borosilicate glass composing typical pharmaceutical vials.
In conventional SFD, the vials are often tightly packed and have approximately the same temperature; consequently, we assumed the vial's lateral wall to be adiabatic and imposed a *Thermal insulation* boundary condition (bc). At the top of the vial, however, heat is transferred from the upper shelf through radiative heat transfer, which was solved using the *Surface-to-Ambient Radiation* bc, imposing the shelf temperature as the *Ambient Temperature*. Here we assumed a glass emissivity equal to 0.9 and a view factor of 1. Consequently, the heat arriving from the upper shelf produces a temperature increment in the vial top, resulting in a cascade heat transfer to the packed bed top layer. In this model, we accounted for this effect imposing another radiative heat transfer bc on the bed top layer and assuming a view factor equal to 1 between the two entities (emissivity of the packed bed equal to 1). The temperature evolution of the vial top was monitored through an *Average Nonlocal Coupling* and used as the heat source in the definition of the bc.
On the other hand, at the bottom of the packed bed, heat is transferred from the shelf through a series of mechanisms (i.e. contact, gas conduction and irradiation). Nonetheless, they can be incorporated in a global heat transfer coefficient[4], K_v', proportional to the chamber pressure, and accounted for using a *Heat Flux* bc, imposing the shelf temperature as the source temperature.
In the packed bed domain, the energy balance reads:

$$\rho_{bed} c_{p,bed} \frac{\partial T_{bed}}{\partial t} = \nabla(k_{bed} \nabla T_{bed}) - c_{p,gas}\left(\nabla(\mathbf{N}_t T_{bed})\right) + \dot{Q} \quad (1)$$

Where ρ, c_p and k are respectively the density, specific heat capacity and thermal conductivity of the materials, while T is the temperature. This equation accounts for heat accumulation, conduction, convection and generation. Here, $\dot{Q}$ is the volumetric heat generation (or absorption) due to sublimation while the term $\mathbf{N}_t$ represents the total gas mass flux in the porous matrix.
The physical properties of the packed bed, modeled as a pseudo-homogeneous medium, were approximated as a linear combination of the frozen and dried particles and the gas occupying the interstices, weighted on their corresponding volumes, which is proportional to the ice-saturation, S. The value of S was defined, locally, as the ratio between the amount of sublimated ice, $C_{ice,sub}$, and the initial ice content, $C_{ice,0}$:

$$S = 1 - \frac{C_{ice,sub}}{C_{ice,0}} \quad (2)$$

The initial ice content depends on the bed and particles porosities (respectively ε_{bed} and ε_p) and can be calculated as:

$$C_{ice,0} = \frac{(1-\varepsilon_{bed})\varepsilon_p \rho_{ice}}{M_w} \quad (3)$$

Where M_w is the water molecular weight and ρ_{ice} the ice density.
The term $\dot{Q}$ was simulated adding a volumetric *Heat Source* to the packed bed domain, and defined as:

$$\dot{Q} = -G_w \Delta H_s M_w \quad (4)$$

Where ΔH_s is the ice heat of sublimation and G_w is the volumetric ice sublimation rate (or vapor condensation rate) expressed in mol $m^{-3}s^{-1}$.

Mass transfer

The total mass flux, $\mathbf{N}_t$, is the sum of the water vapor ($\mathbf{N}_w$) and inert gas ($\mathbf{N}_{in}$) mass fluxes and was modeled using the Dusty Gas Model (DGM) [5]. For each component *i*, the mass flux reads:

$$\mathbf{N}_i = \frac{M_i}{RT}(c_1 \nabla p_i + c_2 y_i \nabla P + c_3 p_i \nabla P) \qquad (5)$$

Where the total pressure P is the sum of the water and inert partial pressures, R is the gas constant, y_i the *i*-species molar fraction and c_1, c_2 and c_3 are coefficients accounting respectively for: Knudsen diffusion, bulk binary diffusion, and viscous flow (described with the Darcy's law). The coefficients definition is detailed elsewhere[3], but they were included in COMSOL defining manually the diffusivity coefficients and the convective velocity field inside the *fluid* section of the *Transport of diluted species in porous media* module.

As the ice sublimation (or condensation) proceeds, vapor is generated (or eliminated) inside the packed bed. For this reason, we added a *Species Source* to the product domain, which was equal to G_w. The magnitude of G_w was evaluated assuming a local non-equilibrium between the ice-vapor equilibrium pressure at the particles sublimating interface, p_{ice}^0 and the concentration of water vapor in the empty inter-particle space:

$$G_w = \left(\frac{p_{ice}^0(T)}{RT} - C_w\right) v \qquad (6)$$

In this equation, the kinetic parameter v differentiated between the sublimation (v_s) and condensation (v_c) kinetics, based on the sign of the driving force. If, at a certain temperature, the local water vapor concentration was lower than the equilibrium concentration, ice in the particles would sublimate and G_w assumed positive values, while condensation occurred if there was an excess of water vapor in the space surrounding the particles, and G_w became negative. The value of the kinetic parameters was estimated through a mathematical model describing the sublimation of individual particles, as will be described later.

The value of p_{ice}^0 was calculated through an *Analytic Function* defined with the Marti-Mauresberger relationship[6]:

$$\log_{10}(p_{ice}^0) = \frac{-2663.5}{T} + 12.537 \qquad (7)$$

Once the sublimation flux was defined, its integration over time provided the local, total amount of sublimated (or condensed) ice:

$$C_{ice,sub} = \int_0^t G_w dt \qquad (8)$$

Which was then used to calculate S in equation (2. The time integration was performed adding a *Domain ODE and DAE* node and specifying that the derivative of $C_{ice,sub}$ was equal to the source term G_w.

At the top of the packed bed, the concentration of the two mobile species was assumed to be equal to the one of the drying chamber: the water vapor accounted for 95% of the chamber pressure, while inert for the remaining 5%.

Drying of individual particles

The kinetic parameter v_c was estimated simulating the drying behavior of individual particles. The particle was divided in two subdomains, namely the dried layer and the frozen region, divided by a moving interface. For simplicity, only water vapor was considered for the gas phase inside the dried layer. The motion of the moving interface was computed solving the Stefan problem with the *Phase Change Interface* node. The interface temperature to set equal to the ice-vapor equilibrium temperature through (7. Solving the heat balance equation for an infinitesimally thin interface, the interface velocity was:

$$\mathbf{v}_{int} = \frac{\mathbf{n}_{int} \cdot (-k_f \nabla T_f) - \mathbf{n}_{int} \cdot (-k_d \nabla T_d)}{\Delta H_s \rho_{ice} \varepsilon_p} \qquad (9)$$

Where subscripts f and d stood respectively for *frozen* and *dried* and $\mathbf{n}$ was the surface normal versor.

At the interface, sublimation was included adding *mass flux* bc, and it was calculated imposing the continuity condition between the generated vapor and the sublimated ice:

$$-\mathbf{n}_{int} \cdot \mathbf{N}_{w,int} = \mathbf{v}_{int} \rho_{ice} \varepsilon_p \qquad (10)$$

The vapor flow inside the dried layer was described according to the Darcy equation, while the permeability was calculated with the Carman-Kozeny equation[3].

At the particle external surface we defined two boundary conditions. Firstly, the external pressure was set equal to the chamber pressure. Secondly, we defined the inward heat flux assuming that the particle was in contact with the vial bottom and received a portion of the heat flux coming from the shelf, based on the number of particles occupying the vial bottom.

Finally, once the sublimation flux was calculated as a function of time, we evaluated the kinetic parameter v_s integrating the sublimation flux over the interface surface, S_{int}, and dividing it by the driving force and the reference volume, V_{ref}:

$$v_s = \frac{\oiint \mathbf{n}_{int} \cdot \mathbf{N}_{w,int} dS_{int}}{\left(\frac{p_{int}}{RT_{int}} - \frac{P_c}{RT_{r=R_0}}\right) M_w V_{ref}} \qquad (11)$$

$$V_{ref} = \frac{{}^4/_3 \pi R_0^3}{1 - \varepsilon_{bed}} \qquad (12)$$

The parameter v_s, calculated as a function of time, was then correlated to the frozen fraction to obtain a time-independent variable. As the particles dries, the resistance to the mass transport inside the particle

increases, along with the pressure driving force, and the kinetic parameter reduces.
The value of the kinetic parameter was then extracted and used for the simulations of the packed bed.

Model parameters definitions

In order to use the macroscopic model, it was necessary to define some key parameters of the packed bed; specifically, the porosity, permeability, tortuosity and the packed bed pore size. To evaluate these parameters, we performed a SFD experiment and studied the resulting powder. A 5% (w/w) mannitol solution was prepared in water for injection and sprayed at a 5 mL/min flow rate into a Dewar containing liquid nitrogen, by a 60 kHz ultrasonic atomizer. The frozen particles were collected, transferred into 10R glass vials, up to a bed height of 15 mm, and dried under vacuum in a MicroFD®. Primary drying was performed at 10°C and 15 Pa, while secondary drying was conducted at 20°C for 5 h. Subsequently, the powder was characterized using a scanning electron microscopy (SEM), obtaining its particle size distribution.
From the particle size distribution, the packed bed structure was replicated in-silico employing the discrete element method (DEM) implemented in Yade[7], obtaining a realistic packing of spheres. From this structure, a volume containing approximately 200 particles was cut out and used as a reduced Representative Element Volume (REV). The REV geometry was then implemented in OpenFOAM v7 and the flow inside the packing simulated under laminar conditions. From the flow field, the tortuosity was evaluated as the ratio between the volume integral of the velocity in the main direction of flow and the magnitude of the velocity:

$$\tau = \frac{\int U_x dV}{\int \|\mathbf{U}\| dV} \tag{13}$$

Additionally, the permeability was calculated from the Darcy equation, knowing the pressure drop across the bed portion and the surface velocity, which was calculated as:

$$U_S = \|\mathbf{U}\| \frac{A_S}{A_T} \tag{14}$$

Where A_S and A_T are respectively the fluid surface (averaged over the bed height) and the total section surface of the bed.
Moreover, the mesh used to simulate the packed bed served to calculate the bed porosity as:

$$\varepsilon_{bed} = \frac{V_{tot} - V_p}{V_{tot}} = \frac{V_{mesh}}{V_{tot}} \tag{15}$$

Where V_{tot} is the total volume of the box containing the particles, V_p is the total volume occupied by the particles and V_{mesh} is the volume of the meshed region outside the spheres.
Finally, we extracted the full size distribution of the pore sizes in the packed bed. To achieve this result, we used the library Trimesh to operate the voxelization of the geometries created via DEM and then used the Python's library PoreSpy[8] to compute the mean dimension of the pores, $d_{pore,bed}$.

Case studies

At the microscale, we estimated the kinetic sublimation velocity v_s as a function of ratio between the particle diameter and pore size, $X = R_0/R_{pore,p}$, which was varied in the range between 5 and 1000, representative of the system physical boundaries. In fact, for X = 5 the pores diameter is comparable with the particles diameter, reaching the limit for the definition of a particle itself. On the other hand, for values of X>1000, and for particles as the ones obtained in this study (d_p = 32.5 μm), the particle pores diameter would reach values lower than 30 nm, smaller than the critical nucleus dimension during ice nucleation[9].
At the macroscale, we simulated three case studies, each one employing a different sublimation function v_s. The three functions were obtained from the simulations at the microscopic scale, respectively with a value of X = 1000, X = 100 and X = 30. These three values represented three particular states of the system, i.e. the controlling resistance to mass transport in the system was either determined by the particle, e.g. X = 1000, the packed bed, e.g. X = 30, or a combination of both, e.g. X = 100. In all the simulations v_c was kept constant, i.e., 100 s^{-1}.

Simulation Results

Individual particles

From the simulations at the microscale, we determined the relationship between the value of X and the sublimation kinetics. Two extreme scenarios could be outlined. In the case of high values of X (small pores relative to the particles), the dried layer opposed a strong mass transport resistance, resulting in vapor accumulation at the sublimation interface and a consequent temperature increment. In this case, the particle tends to approach the temperature of the heating source and the drying rate is controlled by the mass transfer within the particles. By contrast, if the values of X are small (large pores in small particles), the mass transport resistance is small and the water partial pressure at the sublimating interface approaches the pressure outside the particle. In this situation, the particle temperature equilibrates at the equilibrium temperature determined by the pressure outside the particle and the drying rate is controlled by heat transfer. These scenarios are illustrated in Figure 2a. Furthermore, as v_s is strongly correlated with the particle resistance to vapor flow, it depends on both X and the dried layer thickness (or S) as indicated in Figure 2b.

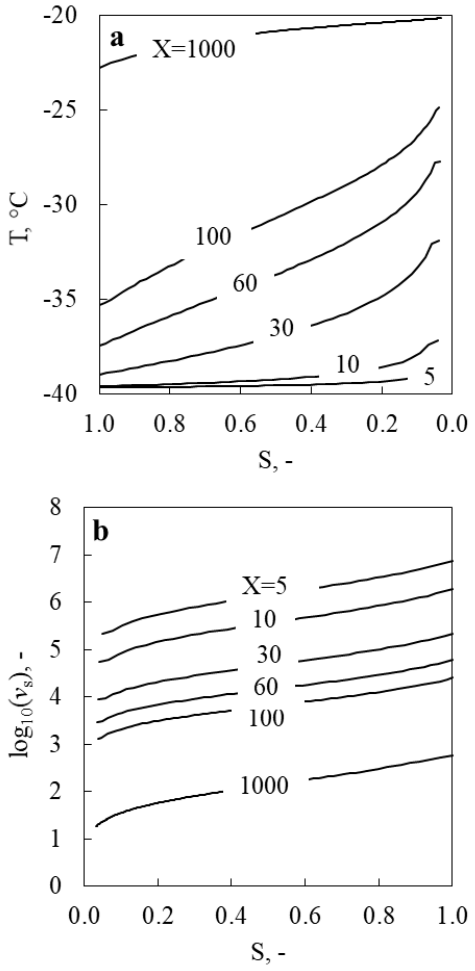

Figure 2. a) *Average particle temperature as a function of X and S.* ***b)*** *Values of the kinetic parameter v_s (in logarithmic scale) as a function of X and S.*

Packed bed simulations

Once all the descriptors of the packed bed were defined, we simulated the drying of the packed bed. Specifically, we investigated three case studies with distinct mass transfer behaviors: the controlling resistance was either determined by the particle, i.e. X = 1000, the packed bed, i.e. X = 30, or a combination of both, i.e. X = 100. Figure 3 illustrates the drying evolution of the packed bed in the case of X = 100.

While the system was described as a pseudo-homogeneous medium, the steep gradient in the ice fraction S allowed to clearly distinguish between the frozen and dried regions. It is important to notice that this distinction was not imposed, but resulted from the process conditions. Moreover, three distinct sublimation fronts formed: one on the top of the packed bed, one on the bottom and one on the side. This condition is tipical of the drying of packed beds but does not occur in conventional freeze drying. In fact, when packed beds are drying, all the particles are in direct contact with the vacuum environment and sublimation may commence regardless of the position in the product domain. Despite receiving approximately the same amount of energy (e.g. ~40-50% of the total entering in the product domain), the upper front moved sensibly faster than the lower front. This condition was determined by the different mass transport resistance offered to each front by the overlaying particles. Lastly, the third front appeared in proximity of the vial wall, which acted as a thermal fin.

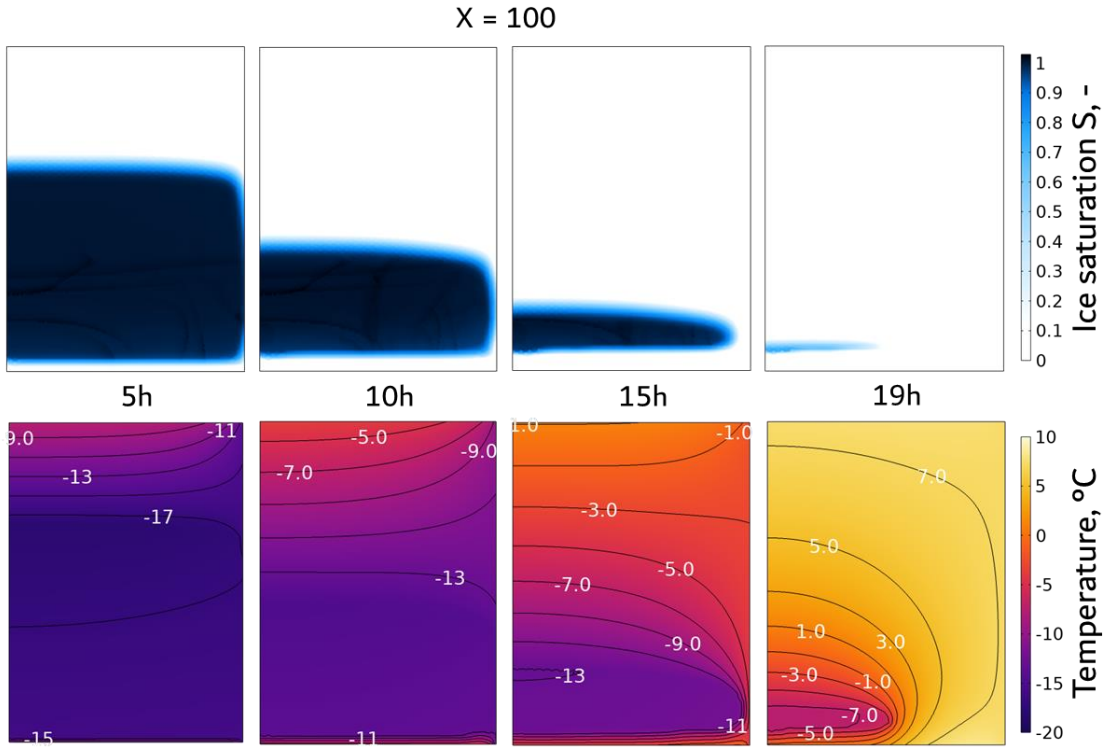

Figure 3. *Evolution of the ice saturation and temperature contour plots of a packed bed of particles having X=100.*

In a packed bed, two mechanisms contribute to the resistance to vapor flow, i.e. the resistance provided by the micro porosity of the particles and the one provided by the macro porosity of the packed bed. For small values of X, e.g. $X \leq 30$, the macro resistance prevailed over the micro resistance and we observed a sharp transition between dried and frozen regions. As Figure 4a illustrates, the diffused interface was localized within a region as thin as 0.1-0.3 mm, corresponding to a few particles lined up. The diffused interface collapsed to a line and the result was very similar to those obtained simulating conventional freeze-drying, where the interface is solved as a Stefan problem. For higher values of X, e.g. X=100, the micro resistance became comparable with the macro resistance and, consequently, the gradient in S became smoother. The diffused interface could be distinguished macroscopically and occupied a significant region of the packed bed as shown in Figure 4b. Eventually, for even higher values of X, e.g. X=1000, the micro resistance controlled the drying rate and ice sublimation occurred uniformly within the packed bed. The diffused interface occupied the whole bed and no clear distinction between dried and frozen regions could be determined, as shown in Figure 4c.

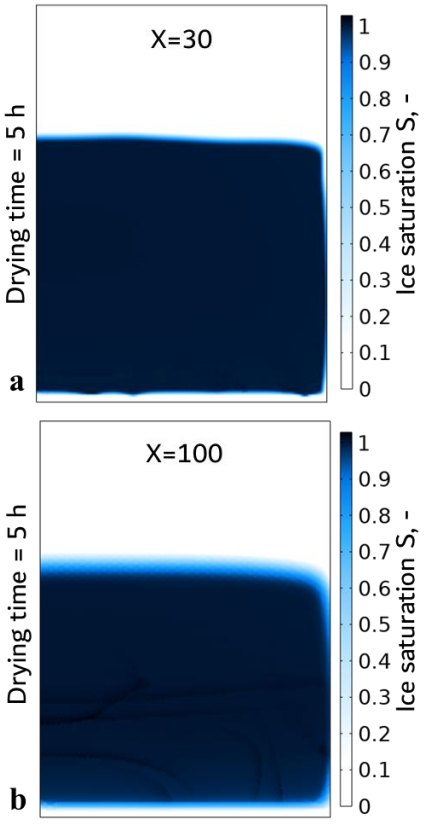

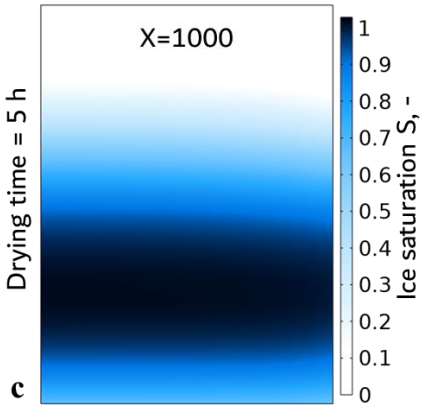

Figure 4. *Ice saturation contour plots after 5h of drying for three packed beds characterized by the same macroscopic parameters with different microscopic structures (indicated by the parameter X.*

Furthermore, the balance between the micro and macro resistance affected the primary drying time and the packed bed temperature as well. In fact, for high X (e.g. X = 1000 in Figure 5a), the value of v_s was small, leading to small sublimation fluxes in the single particles. Macroscopically, this low sublimation rate translated into a low concentration of water vapor in the packed bed, which was expelled from the bed relatively quickly. Consequently, the temperature of the system remained below -10°C and drying ended in about 16 h. On the contrary, for small X (e.g. X = 30 in Figure 5b), the sublimation flux inside the particles was high and water vapour accumulated within the packed bed, which represented the limiting resistance. The water partial pressure increased, resulting in an increment in the packed bed temperature. Since the heating surfaces, i.e. the shelves, maintained a constant temperature throughout the whole primary drying, the heat flux entering the system dropped, resulting in much slower drying, i.e. about 35 h.

For a given particle size distribution and packing of the bed, the fastest drying was obtained by particles with a finer pore size.

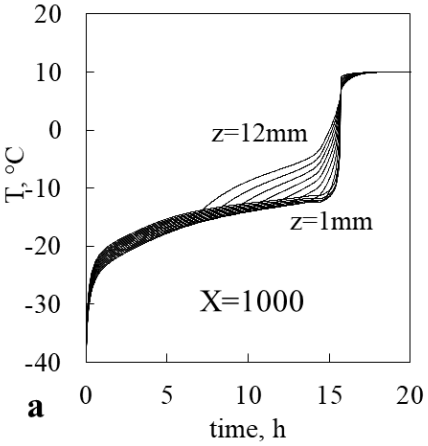

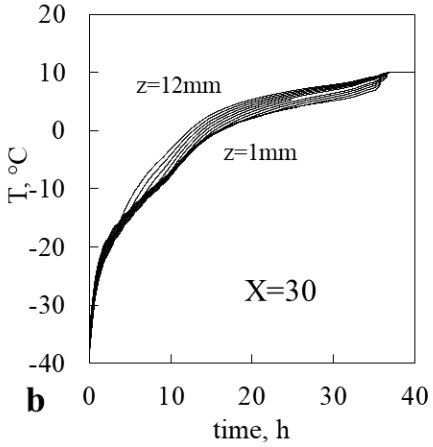

Figure 5. *Temperature profiles of points located at vial centerline and height z varying from 1 mm to 12 mm (each line corresponds to a z increment of 1mm) for packed beds with the same macroscopic structures but different microscopic ones: a) X=1000, b) X=30. Note that in* ***b*** *the x axis is twice as long as the one in* ***a****.*

Conclusions

In this work, we presented a mathematical model to describe the drying behavior of packed beds of spray-frozen particles and its implementation on the software COMSOL Multiphysics. The model is based on the concept of a diffused interface and uses a multiscale approach to obtain the packed bed descriptors. The model can predict different scenarios, depending on the structure of the particles and the packed bed configuration. For instance, in cases of high mass transport resistance inside the packed bed, and low resistance in the individual particles, a steep transition between the dried and frozen particles appears. In opposition, when the resistance inside the single particle is higher than that of the packed bed, sublimation uniformly starts within the entire packed bed, and no sharp transition can be detected. Additionally, the microscopic particle structure influences the drying time as well, with particles presenting big pores resulting in the longest drying times.

The present method overcomes the inaccuracies of the previous ones found in the literature and predicts the development of multiple drying fronts, which could not be detected before.

Despite still requiring a detailed experimental validation, this model serves as a valuable tool for understanding the spray freeze drying process and facilitating its implementation within the pharmaceutical sector.

References

[1] A. I. Liapis and R. Bruttini, “A mathematical model for the spray freeze drying process: The drying of frozen particles in trays and in vials on trays,” *Int. J. Heat Mass Transf.*, vol. 52, no. 1–2, pp. 100–111, Jan. 2009, doi: 10.1016/j.ijheatmasstransfer.2008.06.026.

[2] L. C. Capozzi, A. A. Barresi, and R. Pisano, “A multi-scale computational framework for modeling the freeze-drying of microparticles in packed-beds,” *Powder Technol.*, vol. 343, pp. 834–846, Feb. 2019, doi: 10.1016/j.powtec.2018.11.067.

[3] L. Stratta *et al.*, “A diffused-interface model for the lyophilization of a packed bed of spray-frozen particles,” *Chem. Eng. Sci.*, vol. 275, no. April, p. 118726, Jul. 2023, doi: 10.1016/j.ces.2023.118726.

[4] R. Pisano, D. Fissore, and A. A., “Heat Transfer in Freeze-Drying Apparatus,” in *Developments in Heat Transfer*, InTech, 2011. doi: 10.5772/23799.

[5] E. A. Mason, A. P. Malinauskas, and R. B. Evans, “Flow and Diffusion of Gases in Porous Media,” *J. Chem. Phys.*, vol. 46, no. 8, pp. 3199–3216, Apr. 1967, doi: 10.1063/1.1841191.

[6] J. Marti and K. Mauersberger, “A survey and new measurements of ice vapor pressure at temperatures between 170 and 250K,” *Geophys. Res. Lett.*, vol. 20, no. 5, pp. 363–366, 1993, doi: 10.1029/93GL00105.

[7] Smilauer et al., “Yade Documentation 3rd ed.,” 2021, doi: 10.5281/zenodo.5705394.

[8] J. Gostick *et al.*, “PoreSpy: A Python Toolkit for Quantitative Analysis of Porous Media Images,” *J. Open Source Softw.*, vol. 4, no. 37, p. 1296, May 2019, doi: 10.21105/joss.01296.

[9] G. Bai, D. Gao, Z. Liu, X. Zhou, and J. Wang, “Probing the critical nucleus size for ice formation with graphene oxide nanosheets,” *Nature*, vol. 576, no. 7787, pp. 437–441, Dec. 2019, doi: 10.1038/s41586-019-1827-6.